ABOUT APPLYING DIRECTLY THE ALPHA FINITE ELEMENT METHOD (αFEM) FOR SOLID MECHANICS USING TRIANGULAR AND TETRAHEDRAL ELEMENTS

Nguyen Thoi Trung[1,2]**, Nguyen Xuan Hung**[1,2]
[1] *University of Science, VNU, HCM*
[2] *Ton Duc Thang University, HCM*

Abstract. An alpha finite element method (αFEM) has been recently proposed to compute nearly exact solution in strain energy for solid mechanics problems using three-node triangular (αFEM-T3) and four-node tetrahedral (αFEM-T4) elements. In the αFEM, a scale factor $\alpha \in [0, 1]$ is used to combine the standard fully compatible model of the FEM with a quasi-equilibrium model of the node-based smoothed FEM (NS-FEM). This novel combination of the FEM and NS-FEM makes the best use of the upper bound property of the NS-FEM and the lower bound property of the standard FEM. This paper concentrates on applying directly the αFEM for solid mechanics to obtain the very accurate solutions with a suitable computational cost by using $\alpha = 0.6$ for 2D problems and $\alpha = 0.7$ for 3D problems.

1. INTRODUCTION

For many decades, the constant finite elements such as three-node triangle and four-node tetrahedron are popular and widely used in practice. The reason is that these elements can be easily formulated and implemented very effectively in the finite element programs using piecewise linear approximation. Further more, most FEM codes for adaptive analyses are based on triangular and tetrahedral elements, due to the simple fact that triangular and tetrahedral meshes can be automatically generated. However, these elements possess significant shortcomings, such as poor accuracy in stress solution, the overly stiff behavior and volumetric locking in the nearly incompressible cases.

In the development of new finite element methods, the strain smoothing technique [1] has been applied to the FEM to formulate and develop four smoothed finite element methods (S-FEM) including a cell-based S-FEM (CS-FEM) ([2]-[8]), a node-based S-FEM (NS-FEM) with the upper bound property in strain energy [9, 10], an edge-based S-FEM (ES-FEM) [11] and a face-based S-FEM (FS-FEM) [12]. Each of four new smoothing methods has different characters and advantages.

Recently, an alpha finite element method (αFEM) using 4-node quadrilateral elements has been developed for the purpose of finding the nearly exact solution in strain energy even for the coarse mesh [13]. In addition, making use of the upper bound property of the NS-FEM, the lower bound property of the standard FEM, and the important idea

of the αFEM for the 4-node quadrilateral elements, a novel alpha finite element method using 3-node triangular (αFEM-T3) elements for 2D problems and 4-node tetrahedral elements (αFEM-T4) for 3D problems is proposed [14]. The essential idea of the method is to introduce a scale factor $\alpha \in [0, 1]$ to establish a continuous function of strain energy that contains contributions from both the standard FEM and the NS-FEM [9]. Based on the fact that the standard FEM of triangular and tetrahedral elements is stable (no spurious zero energy modes), and so is the NS-FEM [9], the αFEM will be always stable. This stability ensures the convergence of the solution. Further more, this novel combined formulation of the FEM and NS-FEM makes the best use of the upper bound property of the NS-FEM and the lower bound property of the standard FEM. Using meshes with the same aspect ratio, a unified approach has been proposed to obtain the nearly exact solution in strain energy for a given linear problem. However, the computational cost of αFEM-T3 and αFEM-T4 to find the nearly exact solution in strain energy at α_{exact} is still expensive, because at least two meshes with the same aspect ratio need to be solved in some cases of α before α_{exact} is determined and the final solution is obtained [14].

This paper concentrates on applying directly the αFEM-T3 and αFEM-T4 for solid mechanics to obtain very accurate solutions with a suitable computational cost. We simply use directly $\alpha = 0.6$ for 2D problems and $\alpha = 0.7$ for 3D problems, and the computational procedure is only performed one time. The numerical results show the excellent performance of the αFEM at $\alpha = 0.6$ for 2D problems and $\alpha = 0.7$ for 3D problems comparing to other compared numerical methods.

2. THE IDEA OF THE PRESENT αFEM

2.1. An alpha finite element method for triangular elements (αFEM-T3) for 2D problems

The αFEM-T3 [14] combines both the NS-FEM-T3 and the FEM-T3 by using the scale factor $\alpha \in [0, 1]$. In the NS-FEM-T3, each triangle is divided into three quadrilaterals of equal area and each quadrilateral is used to calculate the contribution to the stiffness matrix of the node attached to the quadrilateral as shown in Fig. 1.
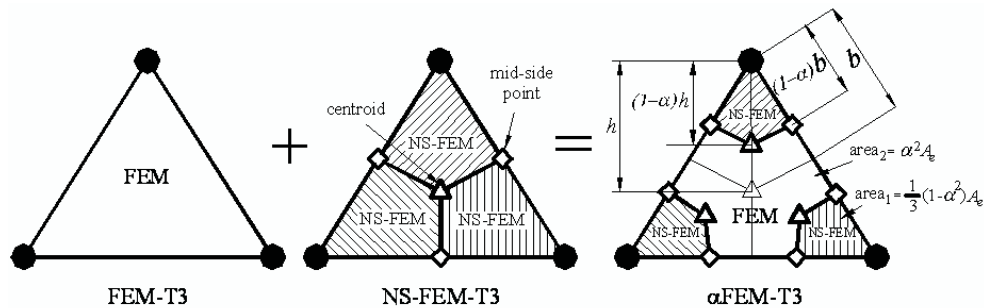
Fig. 1. An αFEM-T3 element: combination of the triangular elements of FEM and NS-FEM. NS-FEM is used for three quadrilaterals, and FEM is used for the Y-shaped area

In the αFEM-T3, the domain V_e of triangular element is divided into four parts with a scale factor α as shown in Fig. 1: three quadrilaterals scaled down by $(1 - \alpha^2)$ at three corners with equal area of $(1 - \alpha^2) V_e/3$, and the remaining Y - shaped part in the middle of the element of area $\alpha^2 V_e$. The NS-FEM-T3 is used to calculate for three quadrilaterals at three corners, while the FEM-T3 is used to calculate for the Y - shaped domain. The entries in sub-matrices of the system stiffness matrix $\mathbf{K}^{\alpha\text{FEM-T3}}$ will be assembled from the entries of those of both NS-FEM-T3 and FEM-T3 as follows

$$\mathbf{K}_{IJ}^{\alpha\text{FEM-T3}} = \sum_{k=1}^{N_n} \mathbf{K}_{IJ(k)}^{\text{NS-FEM-T3}} + \sum_{l=1}^{N_e} \mathbf{K}_{IJ(l)}^{\text{FEM}} \tag{1}$$

where N_n, N_e are the total number of nodes and elements in the whole problem domain and

$$\mathbf{K}_{IJ(k)}^{\text{NS-FEM-T3}} = \int_{\Omega^{(k,\alpha)}} \left(\tilde{\mathbf{B}}_I^{(\alpha)} (\mathbf{x}_k) \right)^T \mathbf{D} \tilde{\mathbf{B}}_J^{(\alpha)} (\mathbf{x}_k) \, d\Omega \tag{2}$$

$$\mathbf{K}_{IJ(l)}^{\text{FEM}} = \int_{\Omega_e^{(\alpha)}} \mathbf{B}_I^T \mathbf{D} \mathbf{B}_J d\Omega = \mathbf{B}_I^T \mathbf{D} \mathbf{B}_J \alpha^2 V_e \tag{3}$$

in which $\mathbf{B}_I = \nabla_s \mathbf{N}_I(\mathbf{x})$ is the *strain-displacement matrix* that produces *compatible* strain fields; $\mathbf{N}_I(\mathbf{x})$ is the shape function of triangular element; $V_e = \int_{\Omega_e} d\Omega$ is the area of the element; $\Omega_e^{(\alpha)}$ is the Y-shape area of triangle; $\Omega^{(k,\alpha)}$ is the area associated the node k and bounded by the boundary $\Gamma^{(k,\alpha)}$ as shown in Fig. 2. The smoothed strain-displacement matrix $\tilde{\mathbf{B}}_I^{(\alpha)} (\mathbf{x}_k)$ for $\Omega^{(k,\alpha)}$ is calculated by

$$\tilde{\mathbf{B}}_I^{(\alpha)} (\mathbf{x}_k) = \frac{1}{V^{(k,\alpha)}} \sum_{i=1}^{N_e^{(k)}} \frac{1}{3} \left(1 - \alpha^2 \right) V_e^{(i)\mathbf{B}_i^e} = \frac{1}{V^{(k)}} \sum_{i=1}^{N_e^{(k)}} \frac{1}{3} V_e^{(i)} \mathbf{B}_i^e = \tilde{\mathbf{B}}_I (\mathbf{x}_k) \tag{4}$$

which implies that we can use the matrix $\tilde{\mathbf{B}}_I (\mathbf{x}_k)$ for area $\Omega^{(k)}$ bounded by the boundary $\Gamma^{(k)}$ instead the matrix $\tilde{\mathbf{B}}_I^{(\alpha)} (\mathbf{x}_k)$ for area $\Omega^{(k,\alpha)}$. In Eq. (4), $N_e^{(k)}$ is the number of elements around the node k; $V_e^{(i)}$ is the area of the ith element around the node k; and $\mathbf{B}_i^e = \sum_{I \in S_i^e}^{\mathbf{B}_I}$ is the compatible strain-displacement matrix of the ith triangular element around the node k. This matrix is assembled from the compatible strain-displacement matrices $\mathbf{B}_I(\mathbf{x})$ of nodes in the set S_i^e containing three nodes of the ith triangular element.

Note that to obtain Eq. (4), the following relation between the area $V^{(k,\alpha)}$ of the domain $\Omega^{(k,\alpha)}$ and the area $V^{(k)}$ of the domain $\Omega^{(k)}$ is used:

$$V^{(k,\alpha)} = \int_{\Omega^{(k,\alpha)}} d\Omega = \sum_{i=1}^{N_e^{(k)}} \frac{1}{3} \left(1 - \alpha^2 \right) V_e^{(i)} = \left(1 - \alpha^2 \right) V^{(k)} \tag{5}$$

Using Eqs.(4) and (5), Eq. (2) now is written as

$$\mathbf{K}_{IJ(k)}^{\text{NS - FEM - T3}} = \left(1 - \alpha^2 \right) \tilde{\mathbf{B}}_I^T \mathbf{D} \tilde{\mathbf{B}}_J V^{(k)} \tag{6}$$
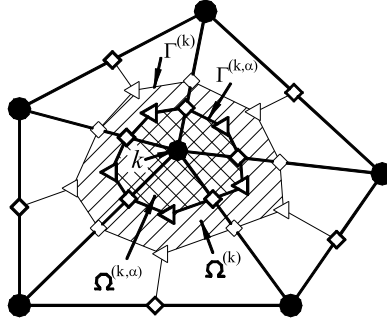
Fig. 2. Cell associated with nodes for triangular elements in the αFEM-T3

which implies that we can simplify the procedure of coding program of the α FEM-T3 by using the original NS-FEM-T3 in which each triangle is only divided into three quadrilaterals of equal area to calculate entries of the stiffness matrix and then multiply $\left(1 - \alpha^2\right)$.

To calculate Eq. (3), the standard FEM using triangular elements is used to calculate the entries of the stiffness matrix and then the parameter α^2 is multiplied.

Now, the αFEM-T3 is equipped with a scaling factor α that acts as a knob controlling the contributions from the NS-FEM-T3 and the FEM. When the factor α varies from 0 to 1, a continuous solution function from the solution of the NS-FEM to that of the FEM is obtained.

2.2. An alpha finite element method for tetrahedral elements (αFEM-T4) for 3D problems

Following the same concept of the αFEM-T3, we develop a tetrahedral element for αFEM for 3D problems (αFEM-T4). The volume V_e of each tetrahedral element will be divided into five parts based on the scale factor α: four volumes at four corners with equal volume of $\left(1 - \alpha^3\right) V_e/4$ and the remaining part in the middle of the element of volume $\alpha^3 V_e$. The NS-FEM is used to calculate for four corner parts of equal volumes, while the FEM-T4 is used to calculate for the remaining volume in the middle. The entries of the system stiffness matrix $\mathbf{K}^{\alpha\text{FEM-T4}}$ is then calculated using

$$\mathbf{K}_{IJ}^{\alpha}\text{FEM-T4} = \sum_{k=1}^{N_n} \mathbf{K}_{IJ(k)}^{\text{NS-FEM-T4}} + \sum_{l=1}^{N_e} \mathbf{K}_{IJ(l)}^{\text{FEM-T4}} \tag{7}$$

with the matrices $\mathbf{K}_{IJ(k)}^{\text{NS-FEM-T4}}$ and $\mathbf{K}_{IJ(l)}^{\text{FEM-T4}}$ calculated as follows:

$$\mathbf{K}_{IJ(k)}^{\text{NS-FEM-T4}} = \left(1 - \alpha^3\right) \tilde{\mathbf{B}}_I^T \mathbf{D} \tilde{\mathbf{B}}_J V^{(k)} \tag{8}$$

$$\mathbf{K}_{IJ(l)}^{\text{FEM - T4}} = \int\limits_{\Omega_e^{(\alpha)}} \mathbf{B}_I^T \mathbf{D} \mathbf{B}_J d\Omega = \mathbf{B}_I^T \mathbf{D} \mathbf{B}_J \alpha^3 V_e \tag{9}$$

in which $\Omega_e^{(\alpha)}$ is the remaining volume in the middle of the element; the smoothed strain matrix $\tilde{\mathbf{B}}_I$, $V^{(k)}$ and the compatible strain-displacement matrix $\mathbf{B}_I$ are calculated by

$$\tilde{\mathbf{B}}_I\left(\mathbf{x}_k\right) = \frac{1}{V^{(k)}} \sum_{i=1}^{N_e^{(k)}} \frac{1}{4} V_e^{(i)} \mathbf{B}_i^e \tag{10}$$

$$V^{(k)} = \int_{\Omega^{(k)}} d\Omega = \frac{1}{4} \sum_{i=1}^{N_e^{(k)}} V_e^{(i)} \tag{11}$$

$$\mathbf{B}_I(\mathbf{x}) = \nabla_s \mathbf{N}_I(\mathbf{x}) \tag{12}$$

where $\mathbf{B}_i^e = \sum_{I \in S_i^e}^{\mathbf{B}_I}$ is the strain-displacement matrix of the ith element around the node k and is assembled from the compatible strain-displacement matrices $\mathbf{B}_I(\mathbf{x})$ of nodes in the set S_i^e containing four nodes of the ith tetrahedral element, $N_e^{(k)}$ is the number of elements around the node k and $V_e^{(i)}$ is the volume of the ith element around the node k.

In the above formulation of the αFEM-T3 (or αFEM-T4), only the area (or volume), the usual compatible strain-displacement matrices $\mathbf{B}_I$ of triangular (or tetrahedral) elements together the factor α are needed to calculate the system stiffness matrix. In the actual programming, the standard FEM and the NS-FEM-T3 (or NS-FEM-T4) formulae are used directly to calculate the entries of the stiffness matrices and then the results obtained are scaled by α^2 and $\left(1 - \alpha^2\right)$, respectively, as shown in Eqs. (3) and (6) for the αFEM-T3 (or by α^3 and $\left(1 - \alpha^3\right)$, respectively, as shown in Eqs. (8) and (9) for the αFEM-T4). Therefore, the αFEM-T3 (or αFEM-T4) code is very similar to a standard FEM code.

Numerical study [14] has shown that using the meshes with the same aspect ratio, the strain energy curves $E\left(\alpha\right)$ corresponding to these meshes will intersect at a common point $\left(\alpha_{\text{exact}}, E_{\text{exact}}\right)$ which gives the nearly exact strain energy of the problem. Note that the meshes with the same aspect ratio were defined in two ways in [14]. Numerical procedure for computing the nearly exact solution at α_{exact} using the αFEM-T3 and αFEM-T4 is summarized in [14]. However, the computational cost of this numerical procedure is still expensive, because at least two meshes with the same aspect ratio need to be solved in some cases of α before α_{exact} is determined and the final solution is obtained.

2.3. About applying directly the αFEM

As seen from the above-mentioned procedure, obtaining α_{exact} requires additional effort, and hence we may want to avoid. Based on the theory presented, we know that in any case, the accuracy (in the strain energy or displacement norm) of an combined model is always better than either FEM or NS-FEM for any $\alpha \in (0, 1)$. This gives us a guarantee that we can only get a better solution using any $\alpha \in (0, 1)$. Therefore as suggested from the numerical results in Refs [14, 15], if we only need to improve the accuracy of solution, we may simply using directly an $\alpha \in [0.5, 0.7]$ in 2D problems and $\alpha \in [0.6, 0.8]$ in 3D problems for any meshes without searching for the α_{exact}. This range of α is found preferable by numerical "experiments" on different linear problems using the αFEM-T3

and αFEM-T4. By this way, the α chosen will not be optimal and the solution may not be very close to the exact one, but the accuracy of the solution is often much better than the FEM using the same mesh.

Specifically in this paper, we simply use directly $\alpha = 0.6$ for 2D problems and $\alpha = 0.7$ for 3D problems for any mesh. The computational procedure is only performed one time and hence the computational cost is not expensive anymore.

3. NUMERICAL EXAMPLES

In order to study the accuracy and convergence rate of the present method, two norms are used here, *i.e.*, displacement norm and energy norm. The displacement norm is given by

$$e_d = \frac{\sum\limits_{i=1}^{N_{dof}} \left| u_i - u_i^h \right|}{\sum\limits_{i=1}^{N_{dof}} \left| u_i \right|} \times 100\% \tag{13}$$

where N_{dof} is the total number of degrees of freedom of problem; u_i is the exact solution and u_i^h is the numerical solution, and energy error norm is defined by

$$e_e\left(\alpha\right) = \left| E\left(\alpha\right) - E_{\text{exact}} \right|^{1/2} \tag{14}$$

where the total strain energy of numerical solution $E\left(\alpha\right)$ is given by

$$\begin{aligned} E\left(\alpha\right) &= E^{\text{FEM}}\left(\alpha\right) + E^{\text{NS - FEM}}\left(\alpha\right) \\ &= \frac{1}{2}\sum\limits_{i=1}^{N_e}\left(\varepsilon_i^h\right)^T \mathbf{D}\varepsilon_i^h \alpha^P V_e^{(i)} + \frac{1}{2}\sum\limits_{k=1}^{N_n}\left(\tilde{\varepsilon}_k^h\right)^T \mathbf{D}\tilde{\varepsilon}_k^h\left(1 - \alpha^P\right)V_n^{(k)} \end{aligned} \tag{15}$$

and the total strain energy of exact solution E_{exact} is calculated by

$$E_{\text{exact}} = \frac{1}{2}\lim_{N_e \to \infty}\sum\limits_{i=1}^{N_e}\varepsilon_i^T \mathbf{D}\varepsilon_i V_e^{(i)} \tag{16}$$

where $P = 2$ for 2D problems and $P = 3$ for 3D problems, ε_i^h is the strain of numerical solution of the ith element, $\tilde{\varepsilon}_k^h$ is the smoothed strain of numerical solution at the kth node, ε_i is the strain of exact solution. In the actual computation using Eq. (16), we will use a very fine mesh $(N_e \to \infty)$ to calculate the "exact" strain energy E_{exact}.

3.1. 2D Cantilever beam under a tip load

A cantilever with length L and height D is studied as a benchmark problem here, which is subjected to a parabolic traction at the free end as shown in Fig. 3.
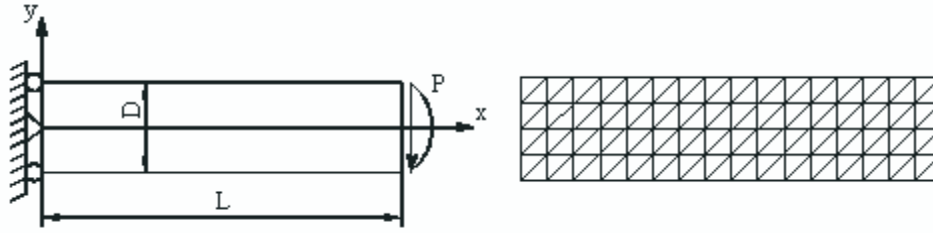
Fig. 3. Model and domain discretization using regular triangular elements of the cantilever

The cantilever is assumed to have a unit thickness so that plane stress condition is valid. The analytical solution is available in a textbook by Timoshenko and Goodier [16].

$$u_x = \frac{Py}{6EI}\left[(6L - 3x)x + (2 + \nu)(y^2 - \frac{D^2}{4})\right]$$
$$u_y = -\frac{P}{6EI}\left[3\nu y^2(L - x) + (4 + 5\nu)\frac{D^2 x}{4} + (3L - x)x^2\right]$$

(17)

where the moment of inertia I for a beam with rectangular cross section and unit thickness is given by $I = D^3/12$. The stresses corresponding to the displacements Eq. (17) are

$$\sigma_{xx}(x, y) = \frac{P(L - x)y}{I}; \quad \sigma_{yy}(x, y) = 0; \quad \tau_{xy}(x, y) = -\frac{P}{2I}\left(\frac{D^2}{4} - y^2\right)$$

(18)

The related parameters are taken as $E = 3.0 \times 10^7 kPa$, $\nu = 0.3$, $D = 12m$, and $P = 1000N$. In the computations, the nodes on the left boundary are constrained using the exact displacements obtained from Eq. (17) and the loading on the right boundary uses the distributed parabolic shear stresses in Eq. (18).

(a)

(b)
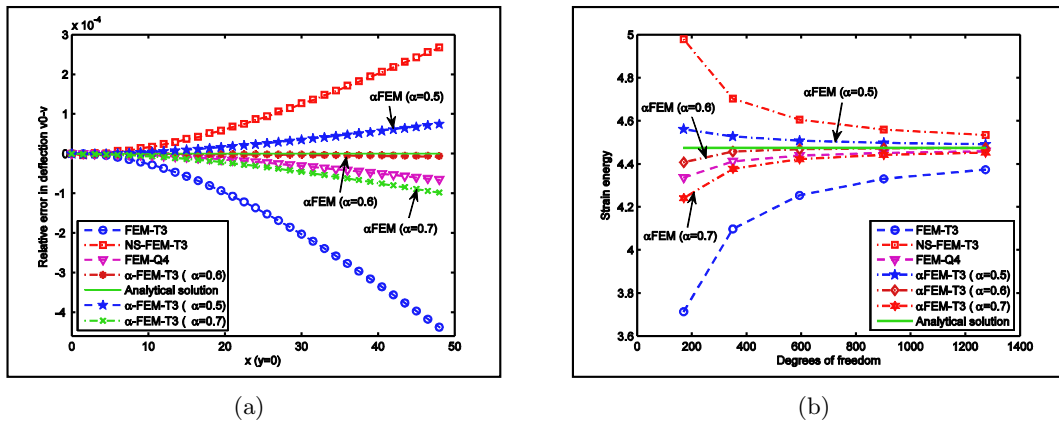
Fig. 4. (a) Relative error in displacement v; (b) Strain energy for the cantilever loaded at the end

One domain discretization of these meshes is shown in Fig. 3. The exact strain energy of the problem is 4.4746. The results of αFEM ($\alpha = 0.6$)are compared with the other methods: the FEM using quadrilateral elements (FEM-Q4), the FEM using triangular elements (FEM-T3), the NS-FEM using triangular elements (NS-FEM-T3) and also the αFEM ($\alpha = 0.5$) and the αFEM ($\alpha = 0.7$).

Fig. 4(a) shows the relative error in deflection along axis x ($y = 0$), and Fig. 4(b) shows the strain energy versus degrees of freedom of methods. Fig. 5(a) and Fig. 5 (b) show the displacement and energy norms of methods, respectively. It is seen that the results of αFEM-T3 ($\alpha = 0.6$)are the best, and even much better than those of FEM-Q4. In addition, the convergence rate of αFEM-T3 ($\alpha = 0.6$) in both displacement norm ($r = 3.52$) and energy norm ($r = 1.87$) are much higher than those of theory ($r = 2$ for displacement and $r = 1$ for energy).

(a)   (b)
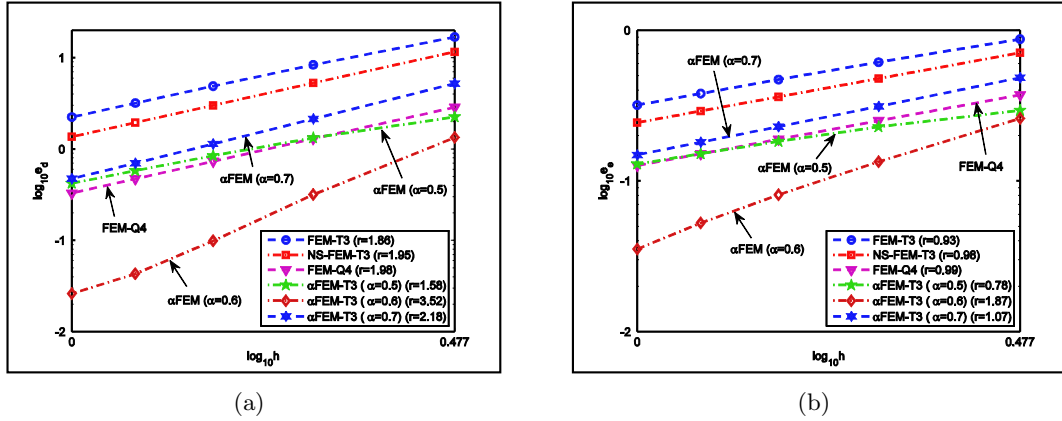
Fig. 5. (a) Displacement norm; (b) Energy norm for the cantilever loaded at the end

Fig. 6 shows that the distribution of the normal and shear stresses using the αFEM-T3 ($\alpha = 0.6$) agree very well with the analytical solution.

3.2. 3-D Lame problem

A 3-D Lame problem consist of a hollow sphere with inner radius $a = 1m$, outer radius $b = 2m$and subjected to internal pressure $P = 1N/m^2$. For this benchmark problem, the analytical solution is available in polar coordinate system by Timoshenko and Goodier [16].

$$u_r = \frac{Pa^3r}{E\left(b^3 - a^3\right)}\left[(1 - 2\nu) + (1 + \nu)\frac{b^3}{2r^3}\right] \tag{19}$$

$$\sigma_r = \frac{Pa^3\left(b^3 - r^3\right)}{r^3\left(a^3 - b^3\right)}; \quad \sigma_\theta = \frac{Pa^3\left(b^3 + 2r^3\right)}{2r^3\left(b^3 - a^3\right)} \tag{20}$$

where r is the radial distance from the centroid of the sphere to the point of interest in the sphere.

As the problem is spherically symmetrical, only one-eighth of the sphere model is shown in Fig. 7(a) and symmetry conditions are imposed on the three symmetric planes.
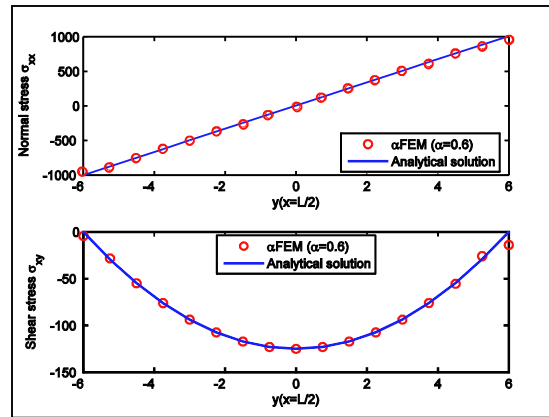
Fig. 6. Numerical results of α-FEM-T3 ($\alpha = 0.6$) and analytical solutions for the cantilever loaded at the end. (a) Normal stress σ_{xx}; (b) Shear stress τ_{xy}

The material parameters of the problem are *E=1.0 kPa* and $v = 0.3$. The exact strain energy of the problem is 6.33e-04. The results of αFEM-T4 ($\alpha = 0.7$) are compared with the other methods: the FEM using hexahedral elements (FEM-H8), the FEM using tetrahedral elements (FEM-T4), the NS-FEM using tetrahedral elements (NS-FEM-T4), and also the αFEM-T4 ($\alpha = 0.6$) and the αFEM-T4 ($\alpha = 0.8$). Fig. 7(b) shows the strain energy versus degrees of freedom of methods.

(a)   (b)
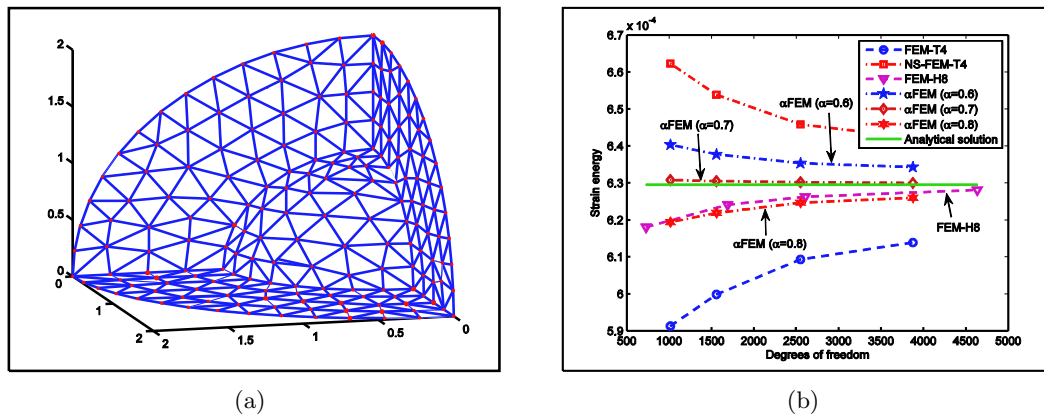
Fig. 7. (a) Discretization of one-eighth of hollow sphere model using 4-node tetrahedral elements; (b) Strain energy for the hollow sphere subjected to inner pressure

Fig. 8(a) and Fig. 8 (b) show the displacement and energy norms of methods, respectively. Again, it is seen that the results of αFEM-T4 ($\alpha = 0.7$) are the best, and even much better than those of FEM-H8. In addition, the convergence rate of αFEM-T4 ($\alpha = 0.7$) in displacement norm ($r = 2.42$) is much higher than those of theory ($r = 2$ for displacement).
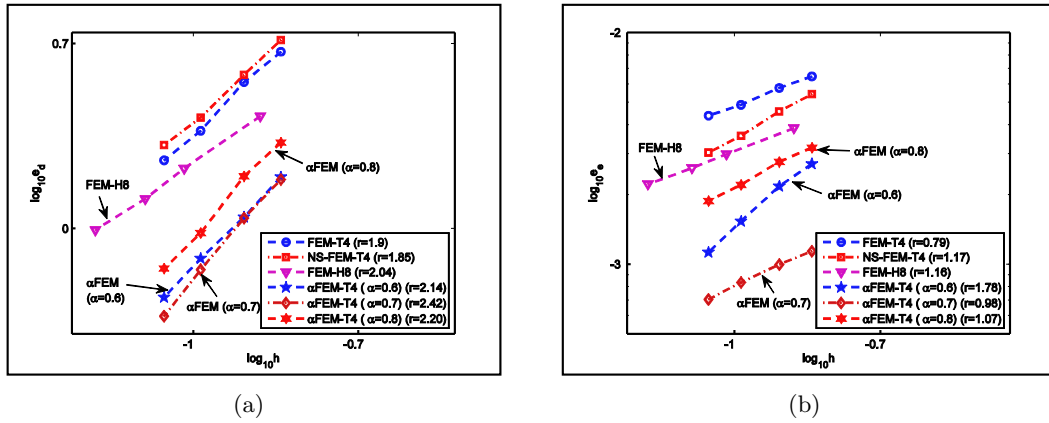
Fig. 8. (a) Displacement norm; (b) Energy norm for the hollow sphere subjected to inner pressure
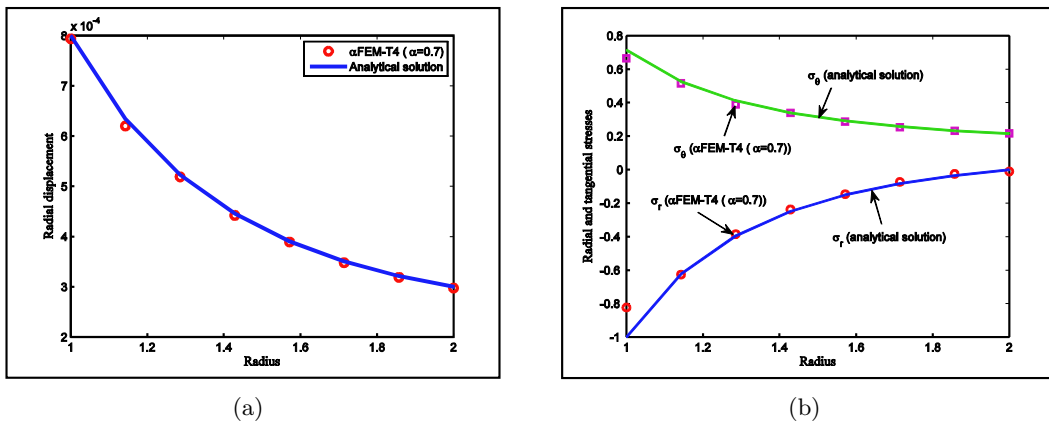
Fig. 9. (a) Radial displacement v; (b) Radial and tangential stresses for the hollow sphere subjected to inner pressure

Fig. 9 shows that the distribution of the radial displacement, radial and tangential stresses using the αFEM-T4 ($\alpha = 0.7$) agree very well with the analytical solution.

4. CONCLUSION

In this work, we apply directly $\alpha = 0.6$ for the αFEM-T3 and $\alpha = 0.7$ for the αFEM-T4 for solids mechanics in 2D and 3D. Through the numerical results, some conclusion can be drawn as follows:

- The results show the excellent performances of the αFEM-T3 ($\alpha = 0.6$) and αFEM-T4 ($\alpha = 0.7$) compared with other compared methods: (1) errors of solutions of the αFEM are much smaller than those of other compared methods; (2) convergence rate of solutions

of the αFEM also converge much faster than those of theory and those of other compared methods.

     - The implementation of αFEM-T3 ($\alpha = 0.6$) and αFEM-T4 ($\alpha = 0.7$) in practical applications is very easy and quite similar to the standard FEM.

     - The obtained result from this study is very promising and the αFEM-T3 ($\alpha = 0.6$) and αFEM-T4 ($\alpha = 0.7$) can be applied directly easily into the available commercial software with little modification.

     - The αFEM-T3 ($\alpha = 0.6$) and αFEM-T4 ($\alpha = 0.7$) is suitable for adaptive analysis as it uses only triangular and tetrahedral elements that can be automatically generated for complicated domains.

REFERENCES

[1] Chen J.S., C.T. Wu, S. Yoon, Y. You, A stabilized conforming nodal integration for Galerkin meshfree method, *International Journal for Numerical Methods in Engineering,* **50** (2000) 435-466.

[2] Dai K.Y., G.R. Liu, T. Nguyen-Thoi, An n-sided polygonal smoothed finite element method (nSFEM) for solid mechanics, *Finite elements in analysis and design,* **43** (2007) 847-860.

[3] Hung Nguyen-Xuan, Stéphane Bordas, Hung Nguyen-Dang, Smooth finite element methods: Convergence, accuracy and properties, *International Journal for Numerical Methods in Engineering*, **74** (2008) 175-208.

[4] H. Nguyen-Xuan, T. Rabczuk, S. Bordas, J.F. Debongnie, A smoothed finite element method for plate analysis, *Computer Methods in Applied Mechanics and Engineering*, **197** (2008) 1184-1203.

[5] Liu G.R., K.Y. Dai, T. Nguyen-Thoi, A smoothed finite element method for mechanics problems, *Computational Mechanics,* **39** (2007) 859-877.

[6] Liu G.R., T. Nguyen-Thoi, K.Y. Dai, K.Y. Lam, Theoretical aspects of the smoothed finite element method (SFEM), *International journal for numerical methods in Engineering*, **71** (2007) 902-930.

[7] T. Nguyen-Thoi, G.R. Liu, K.Y. Dai, K.Y. Lam, Selective Smoothed Finite Element Method, *Tsinghua Science and Technology*, **12(5)** (2007) 497-508.

[8] N. Nguyen-Thanh, T. Rabczuk, H. Nguyen-Xuan, S. Bordas, A smoothed finite element method for shell analysis, *Computer Methods in Applied Mechanics and Engineering*, **198** (2008) 165-177.

[9] Liu G.R., T. Nguyen-Thoi, H. Nguyen-Xuan, K.Y. Lam, A node-based smoothed finite element method for upper bound solution to solid problems (NS-FEM), *Computers and Structures,* **87** (2009) 14-26.

[10] Nguyen-Thoi T, Liu GR, Nguyen-Xuan H, Additional properties of the node-based smoothed finite element method (NS-FEM) for solid mechanics problems, *International Journal of Computational Methods*, **6(4)** (2009) 633-666.

[11] Liu GR, Nguyen-Thoi T, Lam KY, An edge-based smoothed finite element method (ES-FEM) for static, free and forced vibration analyses of solids, *Journal of Sound and Vibration*, **320** (2009) 1100-1130.

[12] Nguyen-Thoi T, Liu GR, Lam KY, Zhang GY, A Face-based Smoothed Finite Element Method (FS-FEM) for 3D linear and nonlinear solid mechanics problems using 4-node tetrahedral elements, *International journal for numerical methods in Engineering*, **78** (2009) 324-353.

[13] Liu G.R, Nguyen-Thoi T, Lam K.Y, A novel FEM by scaling the gradient of strains with factor α (αFEM), *Computational Mechanics*, **43** (2008) 369-391.

[14] Liu G.R., T. Nguyen-Thoi, K.Y. Lam, A novel Alpha Finite Element Method (αFEM) for exact solution to mechanics problems using triangular and tetrahedral elements, *Computer Methods in Applied Mechanics and Engineering*, **197** (2008) 3883-3897.

[15] Liu G.R., Nguyen Thoi Trung, Smoothed Finite Element Methods, *CRC Press, Taylor and Francis Group, NewYork*, (2010).

[16] Timoshenko S.P., J.N.Goodier, Theory of Elasticity (3rd edn), *McGraw-Hill, New York*, (1970).

VỀ VIỆC ÁP DỤNG TRỰC TIẾP PHƯƠNG PHÁP PHẦN TỬ HỮU HẠN VỚI THÔNG SỐ ALPHA (αFEM) CHO CƠ HỌC VẬT RẮN SỬ DỤNG CÁC PHẦN TỬ TAM GIÁC VÀ TỨ DIỆN

Gần đây, một Phương pháp phần tử hữu hạn sử dụng hệ số alpha (αFEM) đã được thành lập để tìm nghiệm gần như chính xác của năng lượng biến dạng cho các bài toán vật rắn có sử dụng các lưới có thể được tạo một cách tự động cho các miền bài toán bất kỳ. Các phần tử tam giác 3 nút (αFEM-T3) và các phần tử tứ diện 4 nút (αFEM-T4) cùng với 1 hệ số tỷ lệ α được thành lập cho các bài toán trong 2 chiều (2D) và ba chiều (3D) một cách tương ứng. Ý tưởng chính của phương pháp là sử dụng 1 hệ số tỷ lệ để kết hợp mô hình hoàn toàn tương thích của FEM và mô hình tựa cân bằng của phương pháp trơn dựa trên nút (NS-FEM). Việc kết hợp giữa FEM và NS-FEM này nhằm sử dụng tốt nhất đặc tính cận trên của NS-FEM và đặc tính cận dưới của FEM. Bài báo này tập trung vào việc ứng dụng trực tiếp phương pháp αFEM cho cơ rắn để tìm nghiệm rất chính xác nhưng chỉ sử dụng một chi phí tính toán hợp lý bằng cách sử dụng $\alpha = 0.6$ cho các bài toán 2D và $\alpha = 0.7$ cho các bài toán 3D.